The electronic spectrum of the Cs-C11H3 radical

Zhao, D.; Linnartz, H.V.J.; Ubachs, W.M.G.

published in
Journal of Chemical Physics
2012

DOI (link to publisher)
10.1063/1.3681259

document version
Publisher's PDF, also known as Version of record

The electronic spectrum of the C_s-$C_{11}H_3$ radical

Dongfeng Zhao (赵东锋),[1,a] Harold Linnartz,[1,2] and Wim Ubachs[1]
[1]*Institute for Lasers, Life, and Biophotonics, VU University Amsterdam, De Boelelaan 1081, NL 1081 HV Amsterdam, The Netherlands*
[2]*Raymond and Beverly Sackler Laboratory for Astrophysics, Leiden Observatory, University of Leiden, P.O. Box 9513, NL 2300 RA Leiden, The Netherlands*

(Received 13 September 2011; accepted 12 January 2012; published online 6 February 2012)

The electronic gas-phase absorption spectrum of the bent carbon-chain radical, HC_4CHC_6H with C_s symmetry, is recorded in the 595 nm region by cavity ring-down spectroscopy through an expanding hydrogen plasma. An unambiguous spectroscopic identification becomes possible from a systematic deuterium labeling experiment. A comparison of the results with recently reported spectra of the nonlinear HC_4CHC_4H and $HC_4C(C_2H)C_4H$ radicals with C_{2v} symmetry provides a more comprehensive understanding of the molecular behavior of π-conjugated bent carbon-chain systems upon electronic excitation. We find that the electronic excitation in the bent carbon-chain $HC_4CHC_{2n}H$ (n = 1–4) series exhibits a similar trend as in the linear $HC_{2n+1}H$ (n = 3–6) series, shifting optical absorptions towards longer wavelengths for increasing overall bent chain lengths. The π-conjugation in bent $HC_4CHC_{2n}H$ (n = 1–4) chains is found to be generally smaller than in the linear $HC_{2n+1}H$ (n = 3–6) case for equivalent numbers of C-atoms. The addition of an electron-donating group to the bent chain causes a slight decrease of the effective conjugation. © *2012 American Institute of Physics*. [doi:10.1063/1.3681259]

I. INTRODUCTION

Free hydrocarbon-chain radicals with delocalized π-electrons, such as finite polyene (–(CH=CH)$_n$–), polyyne (–(C≡C)$_n$–) chains, and cumulene carbenes ($H_2C(=C)_n$–) are important reactive intermediates in the synthesis of new materials such as π-conjugated polymers, carbon nanotubes, and nanowires.[1–4] These reactive species play a role as precursors in the formation of polycyclic aromatic hydrocarbons (PAHs) and fullerenes in hydrocarbon combustion,[5] in plasma environments,[6–8] in terrestrial processes,[9,10] and in dense interstellar clouds.[11–15] Consequently, experimental and theoretical studies dedicated to the nature and unusual electronic and dynamical properties of reactive π-conjugated hydrocarbon chains have attracted much interest.

Recent improvements in the detection sensitivity of optical techniques have made it possible to record electronic gas-phase spectra of carbon-chain radicals in direct absorption and to study the molecular behavior upon electronic excitation.[16] The majority of these species XC_nY (X, Y = H, N, O…) has a linear carbon-chain structure. Subsequent members of the even $XC_{2n}Y$ (or odd $XC_{2n+1}Y$) chain series have similar electronic configurations. Also several of the spectroscopic parameters depend in a systematic way on the number of C-atoms in the chain, most noticeably the optical absorption wavelength of the electronic origin band in homologous series. This is a consequence of the well known particle-in-a-box behaviour—the longer the chain the more corresponding absorption wavelengths shift to the red.[16–20]

In recent years, several nonlinear planar carbon-chain species have been studied in the gas phase.[21–28] Systematic data for different n-values are available for chains of the form $C_{2n+1}H_3$. It was found that the n = 3–6 species detected in a mass-selective REMPI-TOF experiment[23,24] absorb at very similar energies, and do not shift monotonically with increasing C-atom number. It has become clear that this is at least partially a consequence of the fact that not all the observed spectra correspond to homologues of the same series; the carrier of the C_7H_3 spectrum was unambiguously identified as the 2-(buta-1,3-diynyl)cycloprop-2-ylylidene radical containing a three-member ring,[24] whereas the carriers of the C_9H_3 and $C_{11}H_3$ spectra were determined as nonlinear HC_4CHC_4H and $HC_4C(C_2H)C_4H$ structures with C_{2v} symmetry, respectively.[28] These structures, shown in Figs. 1(a) and 1(b), have similar effective bent chain lengths and consequently absorb at rather comparable wavelengths. Another isomeric structure of $C_{11}H_3$–HC_4CHC_6H with C_s symmetry—has a two-C-atom longer chain length and here an effective redshift is expected. For this reason, in the present work, the optical absorption spectrum of the bent C_s-$C_{11}H_3$ radical has been searched for in the wavelength range to the red with respect to the origin band transition of C_{2v}-C_9H_3.[28] An unambiguous identification of the observed bands is possible by applying deuterium labeling as an effective analytical tool to determine the molecular structure. The observed spectra are compared to spectra previously reported for the symmetric and bent C_{2v}-C_9H_3 and C_{2v}-$C_{11}H_3$[28] series, as wells as for the linear $HC_{2n+1}H$ (n = 3–6) series.[19,29] Based on these experimental findings, the π-conjugation in bent odd-carbon-chain systems will be discussed.

[a]Author to whom correspondence should be addressed. Electronic mail: d.zhao@vu.nl.

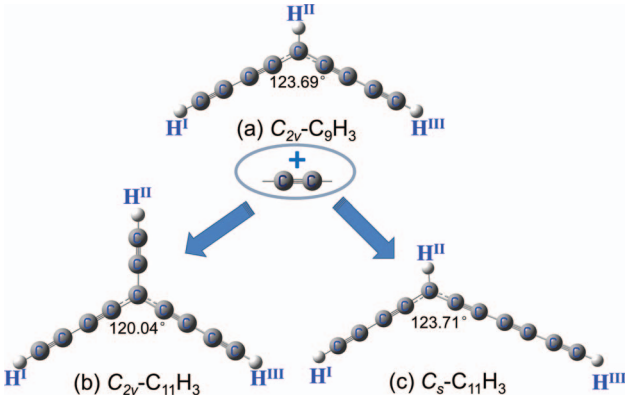

FIG. 1. The molecular structure of (a) C_{2v}-C_9H_3, (b) C_{2v}-$C_{11}H_3$, as derived in Ref. 28 and (c) C_s-$C_{11}H_3$. The angles of bent carbon-chain structures are calculated at the B3LYP/6-311G(d, p) level.

II. EXPERIMENTAL AND THEORETICAL METHODS

A. Experimental setup

Optical spectra of nonlinear carbon chains are recorded by pulsed cavity ring-down spectroscopy through a supersonically expanding hydrocarbon plasma. The experimental setup has been described in detail before.[28,30] Carbon-chain species are produced in a plasma source by discharging an acetylene/helium gas mixture in a pinhole discharge nozzle, which is specifically suitable for the study of larger carbon-chain species. The precursor gas mixture is expanded with a backing pressure of ~10 bar into a vacuum chamber that is pumped by a roots blower system with a total capacity of 1000 m^3/hr. The typical stagnation pressure in the chamber during jet operation amounts to ~0.04 mbar. Three gas mixtures, 0.4% C_2H_2/He, 0.2% C_2D_2/He, and (~0.2% C_2H_2 + 0.15% C_2D_2)/He, are used to create C/H, C/D, and C/H/D plasma jets, respectively. A high voltage pulse (~300 μs and –1200 V) is applied to the electrodes of the discharge nozzle and coinciding with a gas pulse of ~800 μs duration generated by a pulsed valve (General Valve, Series 9) mounted on top of the pinhole discharge body.[28]

The plasma expansion perpendicularly crosses the optical axis of a 58 cm long cavity, approximately 7 mm downstream. This optical cavity consists of two plano-concave mirrors (Research Electro-Optics, two sets of mirrors with reflectivity >99.99% at 580 nm and >99.998% at 532 nm, respectively) mounted on high-precision alignment tools. Cavity ring-down events are obtained by injecting a dye-laser pulse into the high-finesse optical cavity. Light leaking out of the cavity is detected by a photomultiplier tube and typical ring-down times are in the range of 10–20 μs. The setup is operated at 10 Hz, determined by the repetition rate of a Nd: YAG laser (532 nm and 355 nm) that is used to pump the dye laser (Sirah, Cobra-Stretch, bandwidth ~0.06 cm^{-1}). A trigger scheme allows optimizing the timing of the ring-down event with respect to the discharge pulse. The absolute laser frequency is calibrated with an absolute precision better than 0.02 cm^{-1} using an I_2 absorption reference spectrum that is recorded simultaneously.

B. Density functional theory calculations

The analysis of the experimental data is supported by density functional theory (DFT) calculations. The calculations are carried out using the GAUSSIAN 03 software package.[31] Apart from HC_4CHC_2H, all species calculated in this work, including the bent $HC_4CHC_{2n}H$ (n = 2–4) and linear $HC_{2n+1}H$ (n = 3–6) chains, have been theoretically studied previously using smaller basis sets.[32,33] In the present work, these carbon-chain species are (re)calculated at the DFT-B3LYP[34] level with larger basis sets. Specifically, the 6-311G (d, p) basis set is employed for the structural optimization and for the calculation of vibrational frequencies. Previous studies have shown that this basis set predicts rotational constants of conjugated carbon chains with reasonably high precision.[28,33,35] The resulting molecular structures are subsequently employed to predict the vertical electronic transition energy by time-dependent density functional response theory (TD-DFT/B3LYP)[36] employing a 6-311++G(2d, p) basis set. Complete active space multiconfiguration SCF calculations[37] with seven electrons and eight orbitals in the active space (CASSCF(7, 8)) are performed for the bent $HC_4CHC_{2n}H$ (n = 1–4) chains to characterize the role of the active molecular orbitals upon electronic excitation.

TD-DFT predicted values for vertical excitation energies of conjugated hydrocarbons have been argued to be not of highest accuracy because of substantial configuration interaction, while the trend of decreasing excitation energies with increasing chain lengths is nevertheless correctly reproduced.[29,33,38,39] Previous work showed that TD-DFT calculated absorption wavelengths for the bent HC_4CHC_4H species yielded values very comparable to the experimental ones.[28,32] Therefore, for the purpose of this study the TD-DFT/B3LYP method should be sufficiently accurate to predict electronic transition energies for members of the bent $HC_4CHC_{2n}H$ (n = 1–4) chains, and to verify the trend in this homologous series.

III. RESULTS AND ANALYSIS

A. Experimental spectrum of C_s-$C_{11}H_3$

Spectra of the C_s-$C_{11}H_3$ molecule have not been reported so far and here the search for its optical (electronic) absorption spectrum is performed in the 530–620 nm wavelength range by comparing spectra recorded through both C/H and C/D plasma. A strong absorption band is observed at ~16784 cm^{-1} (labeled as h_0) in the C/H plasma, with a corresponding D-isotopically shifted band (labeled as d_0) observed at ~16 828 cm^{-1} in the C/D plasma, as shown in Figs. 2(a) and 2(b), respectively. Besides the bands h_0 and d_0, also two weak bands (labeled as h_1 and d_1 in Fig. 2) are observed in the C/H and C/D plasma, blue shifted by ~27.2 cm^{-1} and 26.3 cm^{-1} with respect to h_0 and d_0, respectively.

Both the h_0 and d_0 bands reflect unresolved P- and R-branch profiles separated by ~1.0 cm^{-1}. A K-stack structure cannot be resolved. The band h_0 in the C/H plasma exhibits a similar band contour as the electronic origin band of C_{2v}-C_9H_3[28] but is ~2100 cm^{-1} (~66 nm) red-shifted. The red-shifted wavelength is close to the value of the observed

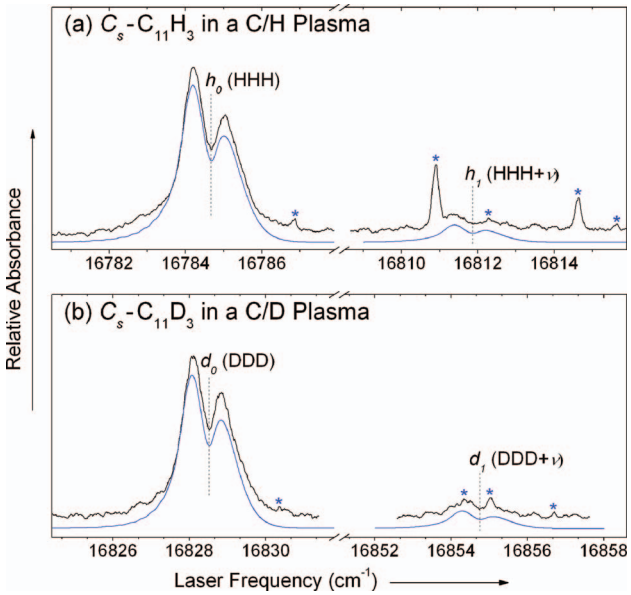

FIG. 2. Experimental spectra of C_s-$C_{11}H_3$ and C_s-$C_{11}D_3$ recorded through: (a) C/H and (b) C/D plasma. The simulated spectra are shown by lower blue traces in each panel. ν denotes the excitation of a low-frequency vibration in the upper electronic state. A rotational temperature of ∼14 K and a Gaussian linewidth of ∼0.1 cm^{-1} are used in the spectral simulations. Irregular features marked by asterisks in both panels are overlapping absorptions from small species, such as C_2, CH/CD… etc.

two-C-atom interval (∼72 nm) in the linear $HC_{2n+1}H$ homologous series.[19,29] Other bands with comparable or larger intensities have not been found in the searched wavelength range. The similar band contour and the red-shift value of band h_0 with respect to the C_{2v}-C_9H_3 electronic origin band are therefore taken as an indication that this band originates from the electronic origin band of C_s-$C_{11}H_3$ (Fig. 1(c)).

A spectral contour fit, assuming an a-type electronic transition for a nonlinear molecule, is applied to the bands h_0 and d_0. This method has been previously used to derive the indicative rotational constants of C_{2v}-C_9H_3 and C_{2v}-$C_{11}H_3$.[28] The fit is performed using the PGOPHER software,[40] and the resulting simulated spectra are shown in the bottom traces of Figs. 2(a) and 2(b), respectively. From the fits, a set of indicative values of the molecular constants

$$A'' \approx 0.15\,\mathrm{cm}^{-1}, \quad B'' \approx C'' \approx 0.009\,\mathrm{cm}^{-1},$$

$$\Delta\left(A - \frac{B+C}{2}\right) = \left(A' - \frac{B'+C'}{2}\right) - \left(A'' - \frac{B''+C''}{2}\right) \approx 0.011\,\mathrm{cm}^{-1}$$

is obtained. The values of the derived rotational constants have a ratio of

$$A'' : \left(\frac{B''+C''}{2}\right) \approx 1 : 0.07,$$

very similar to those found for C_{2v}-C_9H_3,[28] but the absolute values are substantially smaller.

The number and geometrical location of the hydrogen atoms in the carrier of band h_0 is determined by deuterium labeling in a C/H/D plasma jet. A H/D ratio of ∼1:0.8 is used in the C_2H_2/C_2D_2/He gas mixture for the discharge. The recorded spectra are shown in Fig. 3(a). The S/N ratio of the individual spectra is lower than for the pure hydrogenated or deuterated species as the total number of molecules is now shared over several isotopic combinations. In addition, the spectra coincide with overlapping absorption lines of small species, such as C_2, CH/CD… etc. Therefore, in order to inspect the origin of the overlapping absorption lines, additional measurements with a lower backing pressure of ∼2 bar were performed, and the resulting spectra are shown in Fig. 3(b). The experimental conditions with much lower backing pressure in the plasma expansion do not favor the formation of carbon chains, whereas smaller compounds are still present in the plasma. Figure 3(c) shows the resulting spectra by subtracting the overlapping absorption lines due to small carbon species from the spectra displayed in Fig. 3(a), revealing the overlap between spectra of small radicals and long carbon-chain species. Four separated absorption features with unresolved rotational contours can be seen in between or along the h_0 and d_0 bands. These features are ascribed to partially deuterated isotopologue bands of C_s-$C_{11}H_3$.

For large molecules with relatively small rotational constants, the difference between rotational constants of different D-isotopologues is expected to be very small (see the DFT-calculated constants for C_s-$C_{11}H_3$ in Table I as an example). The experimentally derived rotational constants from the fits of bands h_0 and d_0 are therefore also used in the spectral simulations of the individual absorption bands in Fig. 3(c). The simulated spectra, as well as the individual bands, are shown in the middle and lower traces of Fig. 3(c), respectively. From the spectral simulations, in total eight isotopologue bands can be obtained, with quantitatively determined intensity ratios of ∼0.8 : 1 : 0.6 : 0.8 : 0.6 : 0.8 : 0.5 : 0.6, among which the second and seventh band are h_0 and d_0, respectively. The derived band origins are listed in Table I. The estimated uncertainty of the band intensity is less than ±5%. The number of bands is specific for the case of a tri-hydride in which three hydrogen atoms are non-interchangeable (see the supplementary material[42] and Ref. 28 for more details), and consistent with the expected molecular structure of C_s-$C_{11}H_3$. We label the three hydrogen positions in the spectral carrier as H^I, H^{II}, and H^{III} (as indicated in Fig. 1), and employ $H^IH^{II}H^{III}$ as an overall label. Using the band positions derived from the spectral simulation in Fig. 3(c), values for three fundamental H/D isotopic shifts, i.e., H/D isotopic shifts by mono-deuteration of HHH, are determined as ∼30.6 cm^{-1} (Δ^I), −0.7 cm^{-1} (Δ^{II}), and 13.5 cm^{-1} (Δ^{III}), respectively.

B. Structure determination of C_s-$C_{11}H_3$

The ground-state structure of C_s-$C_{11}H_3$ is optimized at the B3LYP/6-311G level. The optimized structure is shown in Fig. 1(c) and the resulting rotational constants are listed in Table I. It is found that the rotational constants of the DFT-calculated C_s-$C_{11}H_3$ structure are in good agreement with the experimentally derived values. Further, TD-DFT calculations predict that C_s-$C_{11}H_3$ has an allowed $1^2A'' - X^2A''$ electronic transition (a-type) with vertical excitation energy of

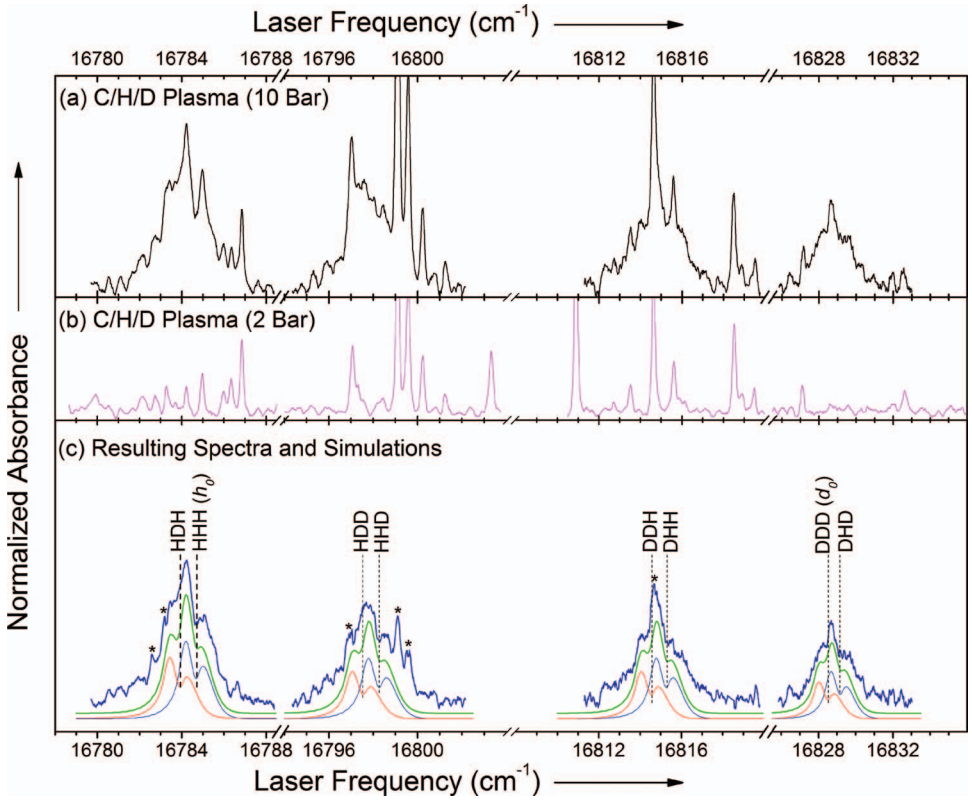

FIG. 3. Experimental spectra recorded through a C/H/D plasma (H/D ratio ∼1:0.8). The backing pressure used for the jet expansion is (a) ∼10 bar and (b) ∼2 bar. The upper blue lines in panel (c) illustrate the resulting spectra of D-isotopologues of C_s-$C_{11}H_3$ by subtracting spectra in panel (b) from panel (a). The simulated spectra are shown by bold green lines in the middle trace of panel (c). The individual simulations of eight D-isotopologues are shown by blue and red lines in the lower traces of panel (c). A rotational temperature of ∼14 K and a Gaussian linewidth of ∼0.1 cm^{-1} are used in the spectral simulations. Irregular features marked by asterisks in panel (c) indicate the residuals of the subtraction.

∼2.20 eV, which is rather close to the experimentally observed absorption band position of h_0 (∼16784.7 cm^{-1}, i.e., 2.08 eV).

From the comparison between the experimental observations and supporting DFT calculations, the assignment of the optical absorption band h_0 to C_s-$C_{11}H_3$, i.e., HC_6CHC_4H (Fig. 1(c)), therefore, is a logical step, even though the present experiment is not mass selective. Furthermore this assignment is consistent with the following observations that are characteristic for a C_s-$C_{11}H_3$ structure:

(1) As discussed in Ref. 28, structural similarities between different unsaturated carbon chains can be derived from their H/D isotopic shifts. The experimentally determined H/D isotopic shifts (see Table I) can be compared to shifts in other carbon chains to further confirm the isomeric structure of C_s-$C_{11}H_3$ as the carrier of the band h_0. It is found that, (a) the experimentally determined fundamental H/D isotopic shifts of band h_0, $\Delta^{I} \sim 30.6$ cm^{-1} and $\Delta^{II} \sim -0.7$ cm^{-1}, are close to the values of $\Delta^{I} \sim 34.9$ cm^{-1} and $\Delta^{II} \sim -1.0$ cm^{-1} for C_{2v}-C_9H_3,[28]

TABLE I. Spectroscopic parameters (in cm^{-1}) of the eight isotopologues of C_s-$C_{11}H_3$.

Isotopologues	DFT/B3LYP-6-311G(d, p)				Expt.			
$(H^{I}H^{II}H^{III})$[a]	A	B	C	ν[b]	T_0	$\Delta_{H/D}$[c]	T_v	ν[d]
HDH	0.1407	0.00886	0.00834	29.5	16784.0(1)	−0.7(1)		
HHH	0.1490	0.00887	0.00838	29.6	16784.71(5)	0.0	16811.9(2)	27.2(2)
HDD	0.1387	0.00864	0.00814	29.1	16797.6(1)	+12.9(1)		
HHD	0.1470	0.00865	0.00817	29.2	16798.3(1)	+13.6(1)		
DDH	0.1357	0.00867	0.00815	28.9	16814.6(1)	+29.9(1)		
DHH	0.1435	0.00868	0.00819	29.0	16815.3(1)	+30.6(1)		
DDD	0.1338	0.00846	0.00796	28.5	16828.55(5)	+43.9(1)	16854.8(2)	26.3(2)
DHD	0.1414	0.00847	0.00800	28.6	16829.2(1)	+44.5(1)		

[a]D-isotopologue formulas are indicated by the permutation $H^{I}H^{II}H^{III}$ instead of $H^{I}C_4CH^{II}C_6H^{III}$.
[b]Values in the ground state, scaled by a factor of 0.968.[41]
[c]Δ denotes the H/D isotopic shift with respect to the main isotopologue HHH, i.e., HC_4CHC_6H.
[d]Experimentally determined values in the electronically excited state.

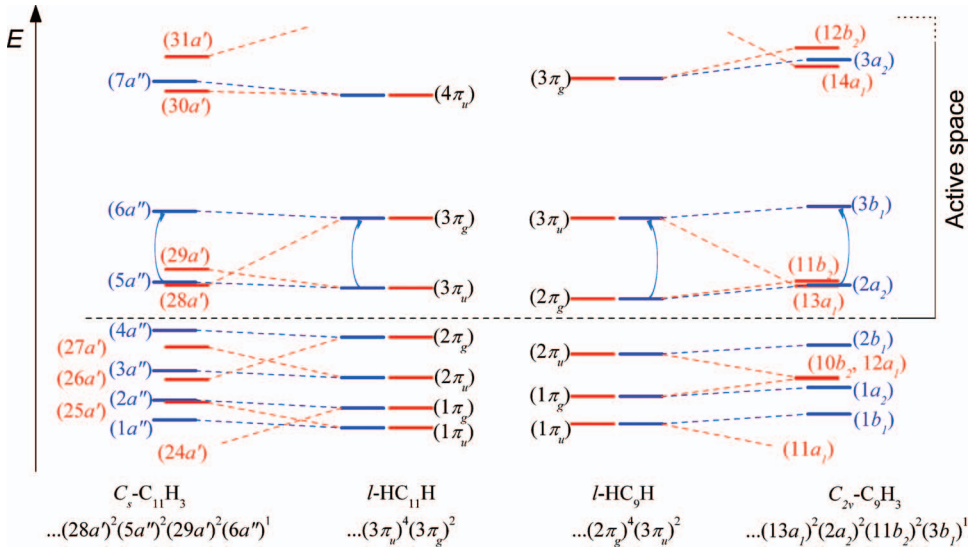

FIG. 4. Schematic diagram of relative molecular orbital energies and correlations between linear and bent nine/eleven-carbon chains. For the bent C_{2v}-C_9H_3 and C_s-$C_{11}H_3$ chains, orbitals colored blue and red are the π-orbitals with orientations perpendicular and parallel to the molecular plane, respectively. The blue arrows denote the electronic excitations as observed in the optical spectra.

indicating that the substructure containing H^I and H^{II} atoms between the spectral carrier of band h_0 and C_{2v}-C_9H_3 must be similar; (b) the value of $\Delta^{III} \sim 13.5$ cm^{-1} is close to the H/D isotopic shift of C_7H ($\sim$19 cm^{-1} for C_7D),[43] indicating that the likely substructure containing H^{III} may be of the form $H^{III}C_6C$-; and (c) the value of $\Delta^{I+III} \sim 44.5$ cm^{-1}, i.e., the H/D isotopic shift of DHD with respect to the main isotopologue HHH, is close to the H/D isotopic shift of $HC_{11}H$ ($\sim$50 cm^{-1} for $DC_{11}D$),[19] indicating that the substructure containing H^I and H^{III} is likely a bent H^I-C_{11}-H^{III} chain. As illustrated in Fig. 1(c), all these spectral (and consequently structural) similarities are consistent with an isomeric C_s-$C_{11}H_3$ structure.

(2) Two weak bands, labeled as h_1 and d_1 in Fig. 2, are observed in the C/H and C/D plasma, and $\sim$27 cm^{-1} blue shifted with respect to the bands h_0 and d_0. These bands are assigned as vibronic transitions involving excitation of the lowest-frequency vibrational mode in the upper electronic state of C_s-$C_{11}H_3$ and C_s-$C_{11}D_3$. Generally, for both linear and non-linear carbon-chain species, the lowest-frequency vibration (C$\cdots$C$\cdots$C bending mode) depends on the overall chain length, as well as the bend angle (see supplementary material[42]). Here the experimentally determined vibrational energy of ν' in the upper state, 27.2 cm^{-1} for C_s-$C_{11}H_3$ and 26.3 cm^{-1} for C_s-$C_{11}D_3$, is $\sim$10 cm^{-1} lower than the experimental values found for C_{2v}-C_9H_3 and C_{2v}-C_9D_3,[28] respectively. Further, the difference between the experimentally determined upper state vibrational energies and DFT-predicted ground-state values is $\sim$9% (see Table I, and Fig. S1 in the supplementary material[42]), nearly the same as that in C_{2v}-C_9H_3.[28] This is consistent with the fact that the bend angle ($\sim$123.7°) in C_s-$C_{11}H_3$ is nearly the same as for C_{2v}-C_9H_3 but the overall chain length of the former molecule is longer by two-C atoms.

(3) The $\sim$67 nm red-shift of band h_0 with respect to the electronic origin band of C_{2v}-C_9H_3, is very close to the TD-DFT predicted value ($\sim$65 nm) (see Table S3 in the supplementary material[42]), and also resembles the red-shift ($\sim$72 nm) of the electronic origin band of linear $HC_{11}H$ with respect to HC_9H.[19,29] According to the 'particle-in-a-box' (PIB) model which treats the delocalized π-electron as a particle in a one dimensional box of conjugated hydrocarbon chain,[20,44] similar π-electron excitations in different linear homologous series of conjugated carbon chains should exhibit a similar trend. Molecular orbital (MO) analysis shows that the orbital configurations in the ground state of C_s-$C_{11}H_3$ and C_{2v}-C_9H_3 are very similar. This is summarized in Fig. 4. Specifically, the conjugated π-bonding MOs in the active space of C_s-$C_{11}H_3$ and C_{2v}-C_9H_3 are closely correlated to the degenerated π-orbitals in linear $HC_{11}H$ and HC_9H, respectively. Further, the electronic transitions corresponding to the observed spectra, $1^2A'' - X^2A''$ for C_s-$C_{11}H_3$ and $1^2A_2 - X^2B_1$ for C_{2v}-C_9H_3, have similar $\pi \leftarrow \pi$ electronic excitations as in the $A^3\Sigma_u^- - X^3\Sigma_g^-$ transitions of linear $HC_{11}H$ and HC_9H, respectively. These correlations are consistent with a picture in which the carrier of the band h_0 is a homologue of the conjugated carbon-chain series including C_{2v}-C_9H_3.

All arguments discussed above lead to the conclusion that the spectral carrier of the observed band h_0 must be the C_s-$C_{11}H_3$ radical with a $H^IC_4CH^{II}C_6H^{III}$ structure as illustrated in Fig. 1(c).

IV. DISCUSSION

A. π-conjugation in a bent odd-carbon-chain system

The present results allow a comparison between the electronic origin-band positions of C_s-$C_{11}H_3$, the previously

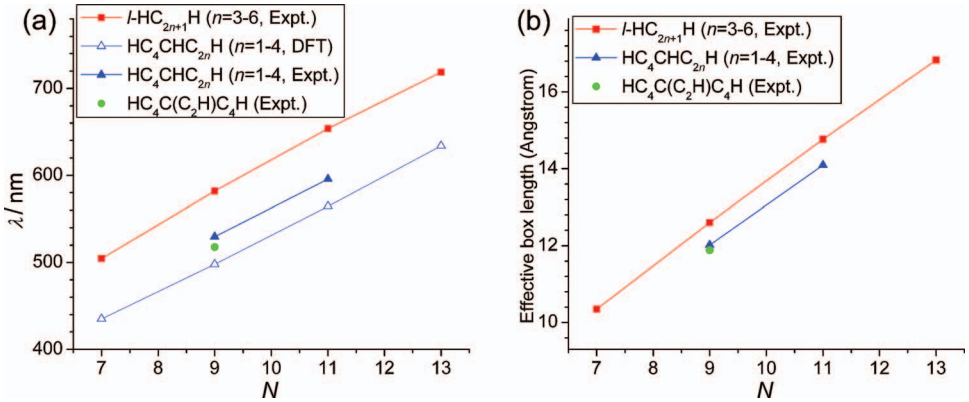

FIG. 5. (a) Calculated and experimentally determined optical absorption wavelengths, (b) effective box length *vs* total number of C-atoms (N) in linear and bent chains. (■: linear $HC_{2n+1}H$ chains for $n = 3$–6 and $N = 2n+1$; ▲ and Δ: bent $HC_4CHC_{2n}H$ chains for $n = 1$–4 and $N = 2n + 5$.) The results of C_{2v}-$C_{11}H_3$ (●: $N = 9$) are also shown in both panels for comparison.

reported bent carbon chains C_{2v}-C_9H_3 and C_{2v}-$C_{11}H_3$,[28] and the linear $HC_{2n+1}H$ (n = 3–6) chains.[19,29] This is summarized in Fig. 5(a). Results of DFT-calculated optical absorption wavelengths for the bent homologous carbon chains $HC_4CHC_{2n}H$ (n = 1–4) are also included in Fig. 5(a). The comparison shows that the optical absorption wavelengths for the bent homologous carbon chains $HC_4CHC_{2n}H$ (n = 1–4) follow an approximate linear relationship, exhibiting a similar trend as in the linear $HC_{2n+1}H$ (n = 3–6) chains.

The MO analysis shows that for bent $HC_4CHC_{2n}H$ (n = 1–4) and linear $HC_{2n+1}H$ (n = 3–6) carbon chains, the MOs in the active space are all π-bonding orbitals formed by combinations of $2p$ orbitals of carbon atoms. These π-orbitals constitute a purely π-conjugation space in which no σ-orbitals are involved. This makes it possible to discuss the π-conjugation in a bent odd-carbon-chain system using the well known PIB model.[44] Using the experimentally observed value of λ_{abs}, the effective box length (L_{eff}) of a conjugated carbon-chain system can be calculated by[42]

$$L_{eff} = \sqrt{\frac{hN_C\lambda_{abs}}{8mc}}, \quad (1)$$

where N_C is the number of conjugated C-atoms. Here, the π-conjugation in the bent carbon-chain system is evaluated in terms of this effective box length L_{eff}.

In Fig. 5(b), it is illustrated that the effective π-conjugation length (L_{eff}) in both linear and bent odd-carbon chains increases quasi-linearly upon increasing the number of π-conjugated C-atoms. In the bent geometric configuration of C_{2v}-C_9H_3 and C_s-$C_{11}H_3$, the effective π-conjugation length is generally somewhat shorter than in the linear geometric configurations of HC_9H and $HC_{11}H$, respectively. This may arise from the change of the hybrid type of the carbon atom at the inflexion point, which is due to typical sp^1 hybridization in a linear carbon chain while it changes to sp^2 hybridization in a ∼120° bent chain structure. DFT calculations show that C_{2v}-C_9H_3 and C_s-$C_{11}H_3$ exhibit nearly the same bend angle of 123.70 ± 0.01°. This angle indicates that compared to linear carbon chains, the combinations of π-MOs in the bent chains involve nearly one less $2p$ atomic orbital, yielding weaker π-conjugation. This is consistent with the fact that the effective π-conjugation lengths (L_{eff}) for the two bent carbon chains undergo similar shortenings compared to linear HC_9H and $HC_{11}H$, respectively. Another possible reason for the smaller effective π-conjugation length in the bent geometric configuration of C_{2v}-C_9H_3 and C_s-$C_{11}H_3$ is that the bent $HC_4CHC_{2n}H$ (n = 1–4) and linear $HC_{2n+1}H$ (n = 3–6) carbon chains have different configuration interactions between their low-lying electronic states. This may affect the effective π-conjugation in highly unsaturated hydrocarbons.

On the other hand, when adding a -C_2-(H^{II}) group in C_{2v}-C_9H_3, the effective π-conjugation length for C_{2v}-$C_{11}H_3$ becomes slightly smaller, as shown in Fig. 5(b). DFT calculations for the charge distribution in C_{2v}-C_9H_3 and C_{2v}-$C_{11}H_3$ show that the -C_2-H^{II} group plays a role as an electron-donating group and provides additional electron density (see Fig. S3 in the supplementary material[42]). As a result, the effective 'one-dimensional-box' length (L_{eff}) slightly decreases.

B. H/D isotopic shifts

In our previous work,[28] it was concluded that the structural similarities between different unsaturated hydrocarbons can be derived from their H/D isotopic shifts. This implies that the H/D isotopic shifts of bent carbon chains like C_{2v}-C_9H_3 and C_s-$C_{11}H_3$ should exhibit a similar behavior as in the case of linear $HC_{2n+1}H$ chains, i.e., the dependence of the H/D isotopic shift on the chain length or the number of C-atoms.[19] Here, similarities between the experimentally determined H/D isotopic shifts of bent C_{2v}-C_9H_3 and C_s-$C_{11}H_3$ chains with shifts compared to linear $HC_{2n+1}H$ (n = 3–6) chains are discussed (see Fig. S4 and Table S4 in the supplementary material[42]).

From the comparison, a similar dependence of the H/D isotopic shift on the overall chain length can be found for both mono- and di-deuteration of the bent chain structure (H^I-$C_4CC_{4(6)}$-H^{III}). Specifically, the values of Δ^{I+III} and Δ^{III} of bent C_{2v}-C_9H_3, and C_s-$C_{11}H_3$ chains exhibit a similar trend as for linear chains with an equivalent number of C-atoms, but their absolute values are slightly smaller. Further, for H^I-deuteration of the same H^I-C_4C substructure in C_{2v}-C_9H_3 and C_s-$C_{11}H_3$, the value of Δ^I also slightly decreases upon increase of the overall bent chain length.

The H/D isotopic shift of the electronic origin band of bent carbon chains also depends on the position of deuteration in the molecule. For example, in the case of the bent carbon chains C_{2v}-C_9H_3, C_{2v}-$C_{11}H_3$, and C_s-$C_{11}H_3$, the value of Δ^{II} from H^{II}/D^{II} substitution is nearly zero, and much smaller than Δ^{I} and Δ^{III} that take values as large as 34.9 cm^{-1}.

The H/D isotopic shift in an electronic transition originates from the change of the vibrational zero-point energy (ZPE) upon electronic excitation, i.e.,

$$\begin{aligned}\Delta^{H/D} &= \Delta(ZPE)^{D} - \Delta(ZPE)^{H} \\ &= \left[\frac{1}{2}\left(\sum_i \nu_i^{D}\right)' - \frac{1}{2}\left(\sum_i \nu_i^{D}\right)''\right] \\ &\quad - \left[\frac{1}{2}\left(\sum_i \nu_i^{H}\right)' - \frac{1}{2}\left(\sum_i \nu_i^{H}\right)''\right] \\ &= \frac{1}{2}\left(\sum_i \nu_i^{D} - \sum_i \nu_i^{H}\right)' - \frac{1}{2}\left(\sum_i \nu_i^{D} - \sum_i \nu_i^{H}\right)'', \end{aligned} \tag{2}$$

where $'$ and $''$ denote upper and lower electronic states, respectively, and ν_i are the frequencies of all vibrational modes. According to Eq. (2), the value of $\Delta^{H/D}$ comprises contributions from all molecular vibrations and is consequently difficult to predict. The $\Delta^{H/D}$ value, however, reflects the overall change of the molecular structure or substructure upon electronic excitation. It is worth to note that the vibrational motions and electronic excitations of homologues of the same series of carbon chains are always very similar. Larger molecules have more normal vibrational modes and larger ground state ZPEs than smaller molecules. Therefore, the observation of smaller H/D isotopic shifts in longer linear or bent carbon chains implies that the change of the molecular structure upon electronic excitation in longer carbon-chain molecules is generally smaller than in shorter chains. Similarly, for non-linear carbon chains C_{2v}-C_9H_3, C_{2v}-$C_{11}H_3$ and C_s-$C_{11}H_3$, the nearly zero value of Δ^{II} upon H^{II}/D^{II} substitution implies that the H^{II} containing substructures (i.e., C-H^{II}, or C–C≡CH^{II}) nearly do not change upon electronic excitation.

V. CONCLUSION

In conclusion, a new isomer of the $C_{11}H_3$ radical, HC_4CHC_6H with C_s symmetry, has been detected and identified using deuterium labeling in the gas phase. A comparison has been made between the present results and available experimental data for bent HC_4CHC_4H, $HC_4C(C_2H)C_4H$, and linear $HC_{2n+1}H$ (n = 3–6) molecules. The spectroscopic parameters have been interpreted from the perspective of π-conjugations in highly unsaturated carbon chains. The dependence of the H/D isotopic shifts on the chain length or the number of C-atoms in the optical spectra of bent C_{2v}-C_9H_3 and C_s-$C_{11}H_3$ has been discussed as well.

ACKNOWLEDGMENTS

This work is financially supported by the Netherlands Foundation for Fundamental Research of Matter and performed within the context of the Dutch Astrochemistry Network supported by NWO.

[1] H. Shirakawa, Rev. Mod. Phys. **73**, 713 (2001).
[2] X. Zhao, Y. Ando, Y. Liu, M. Jinno, and T. Suzuki, Phys. Rev. Lett. **90**, 187401 (2003).
[3] A. Milani, M. Tommasini, M. D. Zoppo, C. Castiglioni, and G. Zerbi, Phys. Rev. B **74**, 153418 (2006).
[4] T. Ma, Y. Hu, and H. Wang, J. Appl. Phys. **104**, 064904 (2008).
[5] K. H. Homann, Angew. Chem., Int. Ed. **37**, 2434 (1998), and references therein; H. Ritcher and J. B. Howard, Prog. Energy Combust. Sci. **26**, 565 (2000).
[6] T. Fujii and M. Kareev, J. Appl. Phys. **89**, 2543 (2001).
[7] Y. Yamaguchi, L. Colombo, P. Piseri, L. Ravagvan, and P. Milani, Phys. Rev. B **76**, 134119 (2007).
[8] H. C. Thejaswini, A. Majumdar, T. M. Tun, and R. Hippler, Adv. Space Res. **48**, 857 (2011).
[9] H. W. Kroto, Int. J. Mass Spectrom. Ion Process. **138**, 1 (1994), and references therein; D. Heymann, L. W. Jenneskens, J. Jehlička, C. Koper, and E. J. Vlietstra, Fullerenes, Nanotubes, Carbon Nanostruct. **11**, 333 (2003).
[10] M. C. McCarthy, M. J. Travers, A. Kovács, W. Chen, S. E. Novick, C. A. Gottlieb, and P. Thaddeus, Science **275**, 518 (1997).
[11] Th. Henning and F. Salama, Science **282**, 2204 (1998), and references therein.
[12] P. Thaddeus, M. C. McCarthy, M. J. Travers, C. A. Gottlieb, and W. Chen, Faraday Discuss. Chem. Soc. **109**, 121 (1998), and references therein.
[13] H. S. P. Müller, F. Schlöder, J. Stutzki, and G. Winnewisser, J. Mol. Struct. **742**, 215 (2005).
[14] V. Wakelam, I. W. M. Smith, E. Herbst, J. Troe, W. Geppert, H. Linnartz, K. Öberg, E. Roué, M. Agundez, P. Pernot, H. M. Cuppen, J. C. Loison, and D. Talbi, Space Sci. Rev. **156**, 13 (2010), and references therein.
[15] P. Ehrenfreund and B. H. Foing, Science **329**, 1159 (2010), and references therein.
[16] E. B. Jochnowitz and J. P. Maier, Annu. Rev. Phys. Chem. **59**, 519 (2008), and references therein; R. Nagarajan, and J. P. Maier, Int. Rev. Phys. Chem. **29**, 521 (2010), and references therein.
[17] P. Freivogel, J. Fulara, D. Lessen, D. Forney, and J. P. Maier, Chem. Phys. **189**, 335 (1994).
[18] J. P. Maier, Chem. Soc. Rev. **26**, 21 (1997), and references therein.
[19] C. D. Ball, M. C. McCarthy, and P. Thaddeus, Astrophys. J. **523**, L89 (1999); J. Chem. Phys. **112**, 10149 (2000).
[20] H. Kuhn, Helv. Chim. Acta **31**, 1441 (1948).
[21] M. C. McCarthy and P. Thaddeus, Chem. Soc. Rev. **30**, 177 (2001).
[22] T. Pino, F. Güthe, H. Ding, and J. P. Maier, J. Phys. Chem. A **106**, 10022 (2002).
[23] T. W. Schmidt, A. E. Boguslavskiy, T. Pino, H. Ding, and J. P. Maier, Int. J. Mass. Spectrom. **228**, 647 (2003); T. W. Schmidt, H. Ding, A. E. Boguslavskiy, T. Pino, and J. P. Maier, J. Phys. Chem. A **107**, 6550 (2003).
[24] H. Ding, T. Pino, F. Güthe, and J. P. Maier, J. Am. Chem. Soc. **125**, 14626 (2003).
[25] M. Araki, H. Linnartz, P. Cias, A. Denisov, J. Fulara, A. Batalov, I. Shnitko, and J. P. Maier, J. Chem. Phys. **118**, 10561 (2003); D. Khoroshev, M. Araki, P. Kolek, P. Birza, A. Chirokolava, and J. P. Maier, J. Mol. Spectrosc. **227**, 81 (2004).
[26] M. Araki, T. Motylewski, P. Kolek, and J. P. Maier, Phys. Chem. Chem. Phys. **7**, 2138 (2005).
[27] H. Ding, A. E. Boguslavskiy, and J. P. Maier, Phys. Chem. Chem. Phys. **7**, 888 (2005).
[28] D. Zhao, N. Wehres, H. Linnartz, and W. Ubachs, Chem. Phys. Lett. **501**, 232 (2011); D. Zhao, M. A. Haddad, H. Linnartz, and W. Ubachs, J. Chem. Phys. **135**, 074201 (2011).
[29] H. Ding, T. W. Schmidt, T. Pino, A. E. Boguslavskiy, F. Güthe, and J. P. Maier, J. Chem. Phys. **119**, 814 (2003).
[30] D. Zhao, M. A. Haddad, H. Linnartz, and W. Ubachs, J. Chem. Phys. **135**, 044307 (2011).
[31] M. J. Frisch *et al.*, GAUSSIAN 03, Revision B.04, Gaussian, Inc., Pittsburgh, PA (2003).
[32] C. Zhang, J. Chem. Phys. **121**, 8212 (2003).

[33]C. Zhang, Z. Cao, H. Wu, and Q. Zhang, Int. J. Quantum Chem. **98**, 299 (2004).
[34]A. D. Becke, J. Chem. Phys. **98**, 5648 (1993).
[35]N. Wehres, D. Zhao, W. Ubachs, and H. Linnartz, Chem. Phys. Lett. **497**, 30 (2010).
[36]M. E. Casida, C. Jamorski, K. C. Casida, and D. R. Salahub, J. Chem. Phys. **108**, 4439 (1998).
[37]F. Bernardi, A. Bottini, J. J. W. McDougall, M. A. Robb, and H. B. Schlegel, Faraday Symp. Chem. Soc. **19**, 137 (1984).
[38]C. P. Hsu, S. Hirata, and M. Head-Gordon, J. Phys. Chem. A **105**, 451 (2001).
[39]G. Mpourmpakis, M. Mühlhäuser, G. E. Froudakis, and S. D. Peyerimhof, Chem. Phys. Lett. **356**, 398 (2002); M. Mühlhäuser, J. Haubrich, and S. D. Peyerimhof, Chem. Phys. **280**, 205 (2002).
[40]C. M. Western, PGOPHER, a Program for Simulating Rotational Structure, University of Bristol.
[41]M. P. Andersson and P. Uvdal, J. Phys. Chem. A **109**, 2937 (2005).
[42]See supplementary material at http://dx.doi.org/10.1063/1.3681259 for "Particle-in-a-box" model for an open-shell odd-carbon system, deuterium labeling of a poly-hydride by non-equivalent H/D ratio, the lowest-frequency bending vibration in linear and bent carbon chains, results from supporting DFT calculation, comparisons of the H/D isotopic shifts, and molecular orbital examinations using the atomic orbital basis set.
[43]H. Ding, T. Pino, F. Guthe, and J. P. Maier, J. Chem. Phys. **117**, 8362 (2002).
[44]H. Kuhn, J. Chem. Phys. **16**, 840 (1948); **17**, 1198 (1949).